

## MODIFICATION OF MIXED STRUCTURE TiO<sub>2</sub> NANOPOROUS-NANOTUBE ARRAYS WITH CdS NANOPARTICLE AND THEIR PHOTOELECTROCHEMICAL PROPERTIES

Hedi Surahman, Supriyono, Yuni K Krisnandi and Jarnuzi Gunlazuardi

Departement of Chemistry-University of Indonesia

Kampus Baru UI Depok 12424

E-mail: [hedi1171@ui.ac.id](mailto:hedi1171@ui.ac.id)

Received: 21 October 2014

Revised: 13 February 2015

Accepted: 10 March 2015

### ABSTRACT

**MODIFICATION OF MIXED STRUCTURE TiO<sub>2</sub> NANOPOROUS-NANOTUBE ARRAYS WITH CdS NANOPARTICLE AND THEIR PHOTOELECTROCHEMICAL PROPERTIES.** In this work, a mixed structure TiO<sub>2</sub> with a top nanoporous layer and an underneath highly ordered nanotube arrays layer (TNPs-NTAs) were prepared by anodic oxidation of Ti foil under controlled anodization time in an electrolyte containing fluoride ion, water and ethylene glycol. CdS nanoparticles (NPs) was deposited onto the mixed structure of TiO<sub>2</sub> by Successive Ionic Layer Adsorption and Reaction (SILAR) with an aim toward tuning the photoelectrochemical performance to visible region. The morphology, elemental composition, crystal structure, optical properties and photoelectrochemical performance of TNPs-NTs and CdS modified (CdS/TNP-NTAs) samples were characterized by Field Emission Scanning Electron Microscope (FESEM), Electron Dispersive Spectroscopy (EDS), X-Ray Diffractometer (XRD), Diffuse Reflectance Spectroscopy (DRS) and electrochemical working station respectively. The results indicate that CdS nanoparticles uniformly decorated on top of surface and inner wall of TNPs-NTs sample. No clogging of CdS-NP at the mouth TNPs-NTAs was observed. The CdS/TNP-NTs show an increasing in the visible light adsorption and photocurrent response. Under white light illumination (9.93 mW/cm<sup>2</sup>), we found that the CdS/TNPs-NTAs have an optimum photocurrent density of 1.16 mA/cm<sup>2</sup>, corresponding to energy photoconversion efficiency of 9.75%, which is 7 times higher than that of the bare TiO<sub>2</sub> (TNPs-NTAs). The increase of photocurrent is attributed to the enhancement of charge separation efficiency and improved electron transport.

**Keywords:** TiO<sub>2</sub> Nanotubes, CdS Nanoparticle, Photoelectrochemical, SILAR, Photocurrent

### ABSTRAK

**MODIFIKASI STRUKTUR CAMPURAN TiO<sub>2</sub> NANOPORI-NANOTUBE DENGAN CdS NANOPARTIKEL DAN SIFAT-SIFAT FOTOELEKTROKIMIANYA.** Dalam pekerjaan ini, struktur campuran TiO<sub>2</sub> dengan lapisan nanopori pada bagian atas dan lapisan *nanotube* pada bagian dibawahnya (TNPs-NTAs) di preparasi dengan oksidasi anodik lempeng Ti dibawah kontrol waktu anodisasi dalam larutan elektrolit yang mengandung ion fluorida, air dan etilen glikol. CdS nanopartikel (NPs) dideposisikan pada struktur campuran TiO<sub>2</sub> menggunakan metode *SILAR* dengan tujuan mendapatkan kinerja fotoelektrokimia pada daerah sinar tampak. Morfologi, komposisi elemen, struktur Kristal, sifat optikal dan kinerja fotoelektrokimia sampel TNPs-NT dan CdS/TNPs-NTAs dikarakterisasi dengan *Field Emission Scanning Electron Microscope (FESEM)*, *Electron Dispersive Spectroscopy (EDS)*, *X-Ray Diffractometer (XRD)*, *Diffuse Reflectance Spectroscopy (DRS)* dan peralatan elektrokimia. Hasil karakterisasi mengindikasikan bahwa CdS nanopartikel terdecorasi secara seragam pada permukaan bagian atas dan dinding bagian dalam sampel TNPs-NTAs. Tidak teramati adanya CdS nanopartikel yang menutupi mulut tabung TNPs-NTAs. CdS/TNP-NTAs memperlihatkan peningkatan adsorpsi pada daerah sinar tampak dan respon arus cahaya. Dibawah penyinaran sinar putih (9.93 mW/cm<sup>2</sup>), CdS/TNPs-NTAs mempunyai densitas arus cahaya optimum sebesar 1.16 mA/cm<sup>2</sup>, yang sebanding dengan nilai efisiensi fotokonversi energi 9.75% dan 7 kali lebih besar dibandingkan TNPs-NTAs. Peningkatan arus cahaya dihubungkan dengan efisiensi pemisahan muatan dan transfer elektron.

**Kata kunci:** TiO<sub>2</sub> nanotube, CdS nanopartikel, Fotoelektrokimia, SILAR, Arus cahaya

## INTRODUCTION

In recent years, the issue of energy crisis and environmental pollution problems has driven researchers to develop technologies that can generate clean energy alternative and renewable instead of fossil fuels. The photocatalytic technology seems to be an effective pathway for solving these problems, which was initiated by Fujishima and Honda [1] in 1972 who reported the use of TiO<sub>2</sub> semiconductor photoanode for the photocatalytic water splitting. TiO<sub>2</sub> semiconductor is becoming increasingly attractive for potential applications in energy and environmental fields such as photoelectrochemical (PEC) [2-5], photovoltaic [6-8] and photocatalysis cells [9-10]. For these processes of energy conversion, TiO<sub>2</sub> has shown as a strong candidate owing to its excellent chemical stability, low cost, nontoxicity and environment-friendly feature [2,6,9]. It has been proven that nanostructure TiO<sub>2</sub> electrode has higher photoelectrochemical activity than the bulk form of TiO<sub>2</sub> materials, since bulk TiO<sub>2</sub> suffers from a short diffusion length [11-13]. TiO<sub>2</sub> nanostructures, particularly TiO<sub>2</sub> nanotube arrays (TNTAs) which have one-dimensional channel exhibits good oriented charge-transport property and facilitate the separation of the photo excited charges carriers [11-14]. Since Zwilling et al reported the growth of TNTAs through the electrochemical anodization of Ti foil [15], many investigations to control the tube length, morphology, orientation, wall thickness, and pore diameter on TNTAs have been reported, by adjusting the anodization condition such as anodization voltage [16], electrolyte composition [17], and anodization time [18]. At this time, TNTAs are widely used as photocatalysts [9] and photanodes [5] to effectively harvest sunlight.

However, photocatalytic activity of TiO<sub>2</sub> is limited by its UV-responsive band gap of approximately 3.2 eV, which can only be excited by UV radiation with a wavelength below 390 nm. Therefore, only 5% of the solar light can be utilized by pure TiO<sub>2</sub>. Tremendous efforts have been taken to improve its visible light harvesting ability including dye sensitization [19], doping by metal and nonmetal [20-21], and sensitizing TiO<sub>2</sub> with narrow band gap semiconductor such as CdS [22], CdSe [23], and PbS [24]. CdS semiconductor is an efficient visible light sensitizer for TiO<sub>2</sub> because it has a narrower band gap (2.4 eV) and its conduction band level is 0.5 eV more negative than that of TiO<sub>2</sub>, thus it is widely employed in quantum-dot sensitized solar cell (QDSSCs) [8] and photoelectrochemical cell to hydrogen generation [25].

To date, many methods have been developed to deposit CdS nanoparticles (NPs) on TNTAs such as sequential chemical bath deposition (S-CBD) [26], successive ionic layer adsorption and reaction (SILAR) [25], electrodeposition [27], and using a bifunctional organic linker [28]. Among them, SILAR method is the

most straightforward, and CdS-TNTAs prepared by this method exhibited greatly enhanced photoactivities under visible irradiation [25]. However, when a solution of the CdS precursor is used for preparation of CdS sensitizing TNTAs, the precipitation reaction is often taken place so sudden that lead to formation of large agglomeration of CdS-NPs, which may block the tube's mouths. In addition, the precursor solution tends not to penetrate fully in to the inner side of the TNTAs because of surface tension of the solution [29]. As a result, both the inside tube wall surface and the bottom of the tubes are not fully covered by CdS-NPs, which definitely reduce the photocatalytic performance of photoelectrochemical and solar cells. An effort to avoid the clogging of the CdS-NPs at the nanotube mouth have been reported. Xie et al.[29] and Wang et al.[30] developed a ultrasonication-assisted sequential chemical bath deposition (S-CBD) method and Liu et al. [31] prepared a TNTAs photocatalyst with large intertube spacing and pore size.

In the present work, a mixed structure of TiO<sub>2</sub> with a top nanoporous layer and an underneath highly ordered nanotube layer (TNPs-NTAs) decorated with dispersed CdS-NPs were prepared. The TNPs-NTs were prepared by anodic oxidation Ti foil under control anodization time. While CdS nanoparticles is deposited onto mixed structure TiO<sub>2</sub> by successive ionic layer adsorption and reaction (SILAR). Nanoporous layer with large interporous spacing facilitates the deposition of CdS-NPs on top surface and inner wall TNTAs without clogging at the nanoporous mouth. The photoelectrochemical properties and the stability of modified CdS-TNPs-NTAs under visible light was systematically studied and the results will be discussed.

## EXPERIMENTAL METHOD

### Preparation of TiO<sub>2</sub> Nanotube Arrays

Prior to anodization, the Ti foils (0.2 mm thick, 99.6% purity) were degreased at room temperature by sonicating in acetone and ethanol for 10 min, respectively, then rinsed with deionized water and dried in air. All anodization experiments were carried out in a two-electrode electrochemical cell at room temperature. Ti foils (4 cm x 1.5 cm x 0.02 cm) and stainless steel sheet (5 cm x 1.5 cm x 0.02 cm) were used as the anode and cathode, respectively. The distance between the two electrodes is kept at 1.5 cm in all reported experiments. Ethylene glycol solution containing 0.3 wt% NH<sub>4</sub>F and 2 vol% H<sub>2</sub>O was used as electrolyte. The anodization process was performed with a Direct Current (DC) power supply for 30 minutes. The anodization voltage was 40 V in this study. After electrochemical treatment, the samples were rinsed with deionized water and dried in air. Then the obtained TNTAs were annealed at 450 °C for 2 hours with a heating rate of 2 °C/minutes.

## Preparation of CdS-Sensitized TNTAs by SILAR Method

The CdS-sensitized TNTAs were fabricated by SILAR method. The TNTAs electrode was successively immersed, 1 minute for each step, in 0.05 M  $\text{Cd}(\text{NO}_3)_2$  in ethanol, pure ethanol, 0.05 M  $\text{Na}_2\text{S}$  in methanol, and pure methanol. After methanol washing the electrode was dried in air. This whole procedure is referred to as one full coating cycle. This immersion procedure was repeated for 5, 8, and 10 cycles. The resulting yellow film were dried and then annealed under a nitrogen ( $\text{N}_2$ ) atmosphere at 400 °C for 1 hour.

## Material Characterization

The morphologies of the samples were observed using a Field Emission Scanning Electron Microscope (FE-SEM, Inspec f50, FEI). The element composition was analyzed by electron dispersive spectroscopy (EDAX, Appolo X). The crystalline structure of the samples was identified by X-ray diffractometer using  $\text{Cu K}\alpha$  radiation ( $\lambda=1.5478 \text{ \AA}$ ) (XRD, Philips Analytical). The photoabsorption properties were recorded by an UV-Vis spectrophotometer (UV-Vis 2450, Shimadzu).

## Photoelectrochemical Measurements

Photoelectrochemical measurement were carried out in a three-electrode configuration with the as-prepared sample as the working electrode, Pt mesh as the counter electrode, and saturated  $\text{Ag}/\text{AgCl}$  as the reference electrode in 0.1 M  $\text{Na}_2\text{S}$  aqueous electrolyte. The photoelectrochemical cell consisting of a glass tube with a 2.5 cm diameter and height 5 cm is made of quartz. A computer controlled potentiostat (eDAQ 401) is employed to control the external bias and to record the photocurrent generated. Full spectrum illumination was provided with a 150 W metal halide lamp (Philips Master). The samples are anodically polarized at a scan rate of 25 mV/s under illumination, and the photocurrent is recorded. The photocurrent density versus potential ( $j$ - $V$ ) and photocurrent density versus time ( $j$ - $t$ ) curves of working electrode was carried out by the linear sweep voltammetry (LSV) and multy pulsed amperometry (MVA) methods respectively.

## RESULTS AND DISCUSSION

### Characterization of the Material

Figure 1 shows the FESEM image of the  $\text{TiO}_2$  films prepared by the anodization in an electrolyte solution containing of 0.3 wt %  $\text{NH}_4\text{F}$  and 2 wt % water in ethylene glycol. Anodization voltage was 40 V. Figure 1(a) is the TNTs-NTs which was anodized for 30 minutes, it can be seen that the mixed structure of  $\text{TiO}_2$

with a top nanoporous layer and an underneath highly ordered nanotubes layer (TNTs-NTs) have been observed. The mixed structure is attributed to the fact that the thin nanoporous layer on the top surface of TNTAs is not completely dissolved during the

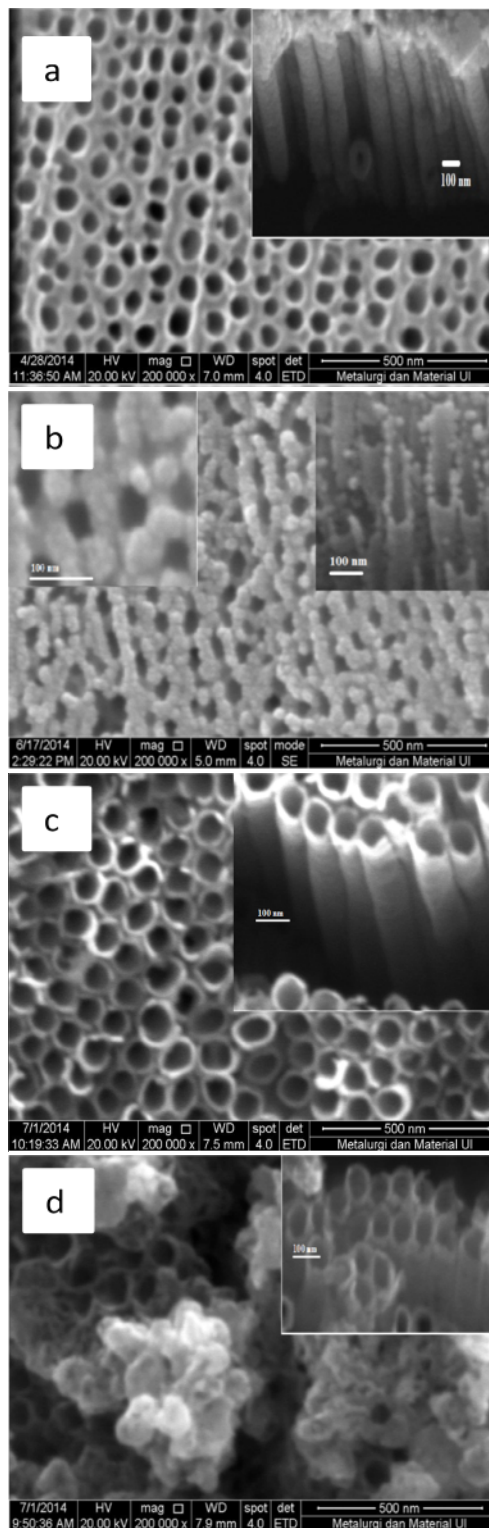
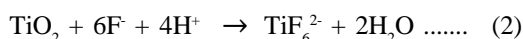
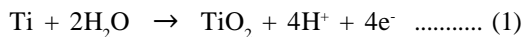


Figure 1. FESEM image of top surface TNTs-NTAs (a). top surface CdS/TNTs-NTAs and high magnification image, (b). top surface TNTAs, (c). top surface CdS/TNTAs and (d). with inset are cross section views

preparation process (30 minutes) in this experiment. While for the anodizing process for 45 minutes, the highly ordered titania nanotubes is completely formed from the top surface to the bottom surface (Figure 1(c)). Based on the TNTAs growth mechanism, anodization process is a competition of electrochemical oxidation (Equation (1)) and chemical dissolution (Equation (2)) [17].



At the initial stage of the anodization, the barrier layer is formed (Eq.1) and it is followed by the appearance of small pits and pore growth in the oxide layer through chemical dissolution reaction (Equation 2). With additional anodization time, the porous structure is converted into a nanotubular structure. Figure 1(b) shows FESEM image of CdS/TNPs-NTs (8cycles), it can be seen that the CdS nanoparticle is uniformly distributed on the top surface nanoporous layer and in the tubes of TiO<sub>2</sub> nanotubes layer. Nanoporous layer with large interporous spacing facilitates the formation of CdS-NPs from Cd<sup>2+</sup> and S<sup>2-</sup> precursors on top surface and inner wall TNTAs without clogging at the nanoporous mouth. While at the TiO<sub>2</sub> nanotube layers, CdS aggregates are clearly observed on the surface of TNTAs layer (Figure 1(d)). In the latter case, the CdS precursor solution could not penetrate deeply into the TNTAs because of the surface tension of the solution, resulting an aggregation at the entrances of the nanotubes [29].

XRD was conducted to characterize the phase structure of both pure TNPs-NTAs and CdS/TNPs-NTAs samples. The phase of TNPs-NTAs was mainly composed of anatase phase after annealing at 450 °C for 2 hours (Figure 2(a)). As shown in Figure 2(b), the peak located at 26.4° and 43.8° were correspondingly attributed to (002) and (110) of the hexagonal CdS (JCPDS No.41-1049), indicating that the deposited CdS layer was hexagonal crystal system.

EDX quantitative analysis of the CdS/TNPs-TNTAs gave an approximately 1:1 stoichiometric ratio of Cd to S (Cd, 2.62%; S, 2.70%), as expected for the format of CdS compound (Figure 3(b)). The atomic ratio of oxygen to Ti (66.39% ; 33.61%) was exactly equal to 2 that was consistent with the stoichiometric formula of TiO<sub>2</sub> (Figure 3(a)).

Figure 4(a) shows the diffuse reflectance absorption spectra of the unmodified and CdS modified samples. TNPs-NTAs without CdS nanoparticles could only absorb UV light below the wavelength of 400 nm and the calculation results using Kubelka-Munk equation shows the band gap value was 3,22 eV (Figure 4(b)), corresponding to the band gap value of anatase phase TiO<sub>2</sub>. For the CdS modified samples with variations in the number of SILAR cycles,

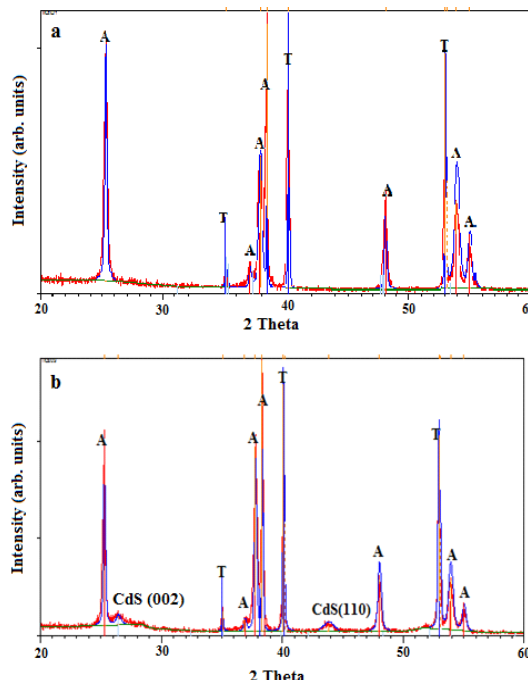


Figure 2. XRD diffractograms of samples: (a). pure TiO<sub>2</sub>, and (b). CdS/TiO<sub>2</sub>, the samples were annealed at 450 °C for 2h

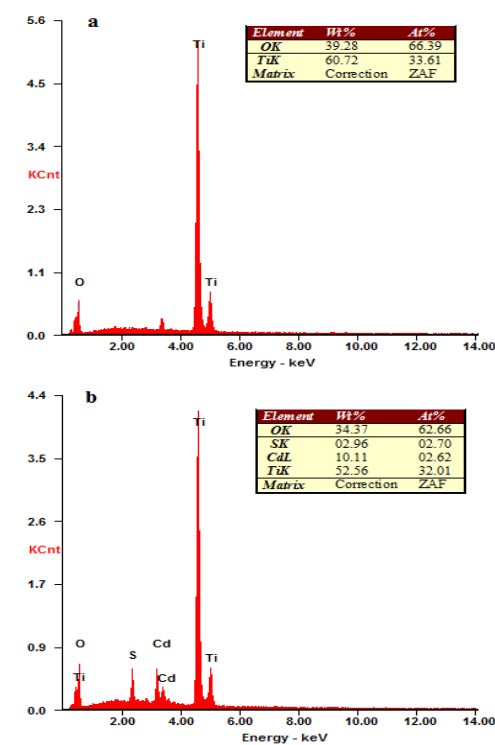


Figure 3. EDX spectrum and the corresponding element constant of (a) pure TiO<sub>2</sub> and (b) CdS/TNPs-TNTAs

a broad absorption band between 400 and 600 nm indicates that the deposition of CdS NPs significantly improves the visible-light absorption property of the TNTAs. The band-gap value of CdS modified samples with 5, 8, and 10 SILAR cycles have a similar values of 2.2eV.

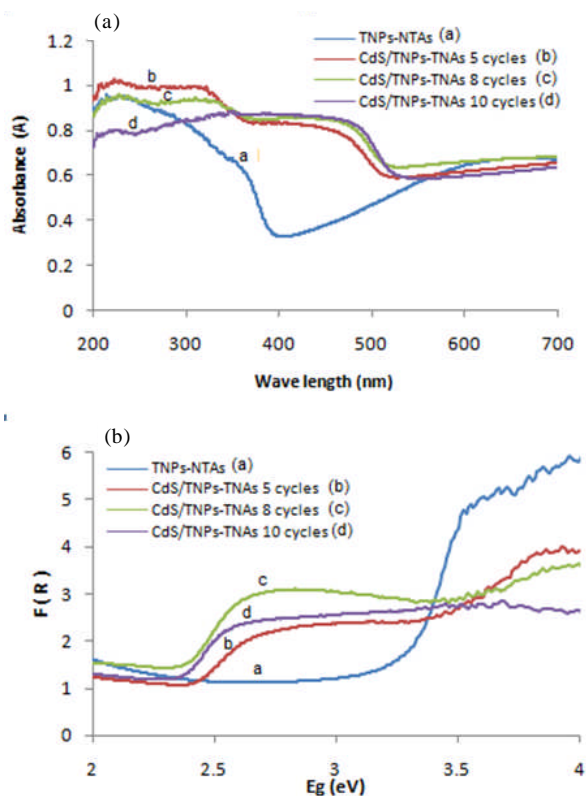


Figure 4. (a). Diffuse reflectance absorption spectra and (b) band gap energy of the unmodified and CdS modified samples

### Photoelectrochemical Properties

Figure 5(a) shows characteristics of the photocurrent density versus potential curve ( $I$ - $V$  curve) for the TNPs-NTAs and CdS/TNPs-NTAs electrode prepared at different deposition cycles. For both the unmodified  $\text{TiO}_2$  and CdS modified  $\text{TiO}_2$  electrodes, the current was observed negligible at dark condition, while under illumination the current density of electrodes were significantly observed. The TNPs-NTAs electrode exhibited a photocurrent of  $0.126 \text{ mA/cm}^2$  at  $0\text{V}$  versus Ag/AgCl, and increased in the presence of CdS, indicating a contribution by the CdS sensitizer. The Maximum value of the photocurrent density of the CdS/NPs-NTAs electrodes depends on the deposition cycle. The CdS/NPs-NTAs electrode which was prepared by 8 deposition cycles have an optimum photocurrent density of  $1.16 \text{ mA/cm}^2$ , which is nearly 9 times higher than the pristine  $\text{TiO}_2$  nanotubes electrode. Increasing deposition cycle results in formation of new crystallites, and crystallite growth. As reported by Kamat et al [11], large nanocrystallite are less efficient in transferring electron than their smaller counterpart. The results of Kalanur et. al [32], show that the increased amount of CdS layer may slow down the electron injection process and an electron will have more chance to be trapped or recombined with holes within CdS layer or alternatively to be captured by an electron acceptor in the

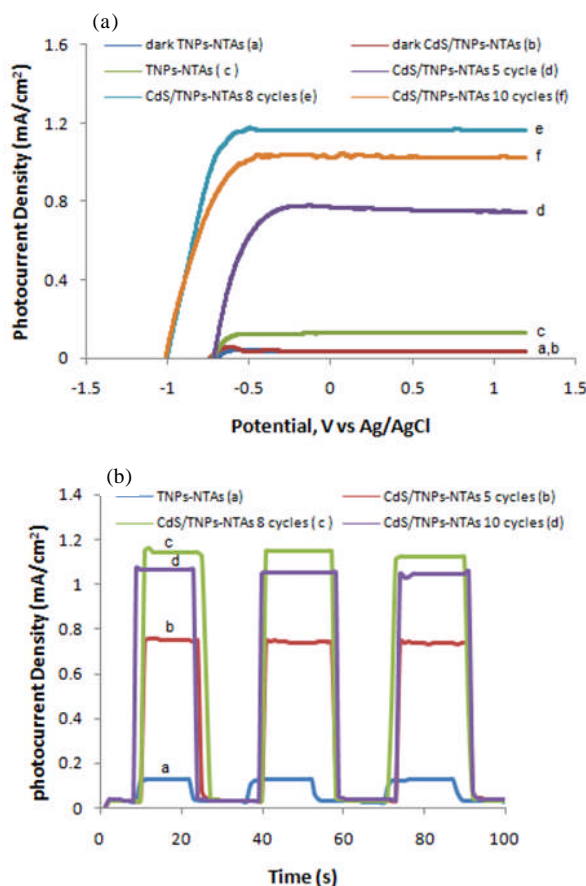
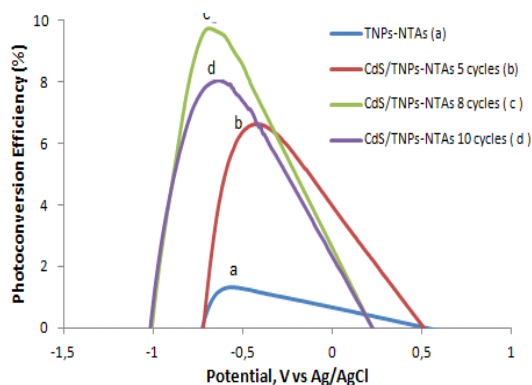


Figure 5. Photoelectrochemical properties of the TNPs-NTAs and CdS/TNPs-NTAs electrodes (a).  $j$ - $V$  curves, (b). time-dependent photocurrents and cycle stability test measured with the potential bias of  $0 \text{ V}$  versus Ag/AgCl under on-off light irradiation

electrolyte. Therefore with increasing deposition cycle, the photocurrent first increase, with CdS sensitization of the  $\text{TiO}_2$  surface, and then decrease as the CdS particle size continuous to increase. As shown in Figure 5(a), the bare  $\text{TiO}_2$  electrode have the open circuit potential (OCP) around  $-0.718 \text{ V}$  and after CdS sensitization by 8 SILAR cycles, this value shifted to around  $-1.012 \text{ V}$ , which indicates a shift in Fermi level to more negative potential as a result of the coupling between  $\text{TiO}_2$  and CdS in the composite system. The more negative potential of Fermi level can enhance of the charge separation and translating into an improvement of the photocurrent response. In the photoelectrochemical system, a higher photocurrent would correspond to a higher efficiency of the PEC device for solar hydrogen generation, as the current is related to the electron needed to reduce the  $\text{H}^+$  ions into  $\text{H}_2$  at the counter cathode.

Figure 5(b) shows the transient photocurrent response of the TNPs-NTAs and CdS/TNPs-NTAs electrodes, which were measured by switching a white light source on and off in  $0.1 \text{ M Na}_2\text{S}$  at an applied potential of  $0 \text{ V}$  in the one-compartment PEC cell by multi pulsed amperometry method. The duration of the light



**Gambar 6.** The corresponding photoconversion efficiency of the TNPs-NTAs and CdS/TNPs-NTAs electrodes

pulse was set at 25 s, followed by dark current measurement for 15 s. As shown in Figure 5(b), the current value is nearly 0 mA/cm<sup>2</sup> in dark condition while the photocurrent rapidly rises to a constant value upon illumination. All photocurrent patterns of TiO<sub>2</sub> samples are highly reproducible and good stability for several light on-off cycles. This result indicates that the CdS modified TiO<sub>2</sub> electrodes prepared by SILAR exhibit good photo response, fast charge transfer and stable photocurrent response.

Figure 6 shows the corresponding photo conversion efficiency ( $\eta$ ) of light energy to chemical energy calculated using the following Equation (5) [25]:

$$\eta(\%) = \frac{j_p \int (E_{rev}^0 - E_{app}) / I_0 dx}{j_p E_{rev}^0} \times 100 \dots\dots\dots (5)$$

where :

- $j_p$  = The photocurrent density (mA/cm<sup>2</sup>)
- $j_p E_{rev}^0$  = The total power output
- $j_p E_{app}$  = The electrical power input
- $I_0$  = The power density of incident light

$E_{rev}^0$  is the standard reversible potential of 1.23 V/NHE that is the potential corresponding to the Gibbs free energy change per photon in the water splitting reaction. The applied potential is  $E_{app} = E_{meas} - E_{aoc}$ , where  $E_{meas}$  is the electrode potential (vs Ag/AgCl) of the same working electrode under open circuit condition in the same electrolyte. The pure TiO<sub>2</sub> such as TNPS-NTAs electrode achieved a photoconversion efficiency of 1.31%. The photoconversion efficiency increased to 9.75% when TiO<sub>2</sub> sensitized by 8 cycles of CdS. The photoactivity value of 9.75% is a 7-fold enhancement compared with that of the pure TiO<sub>2</sub>.

## CONCLUSION

We have demonstrated that the SILAR deposition method of CdS onto a mixed structure TiO<sub>2</sub> electrode with a top nanoporous layer and an underneath highly ordered nanotube layer (TNPs-NTAs) was successfully achieved. This method offers a uniform

distribution and facilitates the deposition of CdS nanoparticles (NPs) on top surface and inner wall TNPs-NTAs sample without clogging of CdS-NPs at the TiO<sub>2</sub> nanoporous mouth. CdS modified TiO<sub>2</sub> electrodes prepared by SILAR exhibit good photo response, fast charge transfer and stable photocurrent response. In comparison with the pure TiO<sub>2</sub> (TNPs-NTAs), the as-prepared CdS/TNPs-NTAs with 8 SILAR cycles shows a 7-fold enhancement in photoconversion efficiency due to narrowing its band gap, hence extend to the visible light response, which is attractive and feasible for its potential application in photocatalytic water splitting.

## ACKNOWLEDGMENTS

The Cluster Research Funding Scheme for The Cluster Research of Solid Inorganic Frame work for Environmental Application (SIFEA) from the University of Indonesia. This work was partially funded by the “Hibah Kolaborasi Luar Negri” scheme from DGHE (DIKTI). The authors would like to thank to Yus Prasetyo for the FESEM measurements.

## REFERENCES

- [1]. A. Fujishima and K. Honda. “Electrochemical photolysis of water at a semiconductor electrode”, *Nature*, vol. 238, pp. 37-38, 1972
- [2]. Y. Li, H. Yu, W. Song, G. Li, B. Yi and Z. Shao. “Novel photoelectrochemical cell with self-organized TiO<sub>2</sub> nanotubes as photoanodes for hydrogen generation”, *International Journal of Hydrogen Energy*, vol. 36, pp. 14374–14380, 2011.
- [3]. Y. R. He, F. F. Yan, H. Q. Yu, S. J. Yuan, Z. H. Tong and G. P. Sheng. “Hydrogen production in a light-driven photoelectrochemical cell”, *Applied Energy*, vol 113, pp. 164-168, 2014
- [4]. Y. Sun, G. Wang and K. Yan. “TiO<sub>2</sub> nanotubes for hydrogen generation by photocatalytic water splitting in a two-compartment photoelectrochemical cell”, *International Journal of Hydrogen Energy*, vol. 36, pp. 15502-15508, 2011
- [5]. C. Carver, Z. Ulissi, C. Ong, S. Dennison, G. Kelsall and K. Helgardt. “Modelling and development of photoelectron chemical reactor for H<sub>2</sub> production”, *International Journal of Hydrogen Energy*, vol. 37, pp. 2911-2923, 2012.
- [6]. P. V. Kamat. “Boosting the Efficiency of Quantum Dot Sensitized Solar Cells through Modulation of Interfacial Charge Transfer”, *Accounts of Chemical Research*, vol. 45, pp. 1906-1915, 2012
- [7]. Y. Lai, Z. Lin, D. Zheng, L. Chi, R. Du, and C. Lin. “CdSe/CdS quantum dots co-sensitized TiO<sub>2</sub> nanotube array photoelectrode for highly efficient solar cells”, *Electrochimica Acta*, vol. 79, pp. 175-181, 2012

- [8]. P. K. Santra and P. V. Kamat. "Tandem-Layered Quantum Dot Solar Cell", *Journal of American Chemistry Society*, vol. 135, pp. 877-885, 2013.
- [9]. J. Liao, S. Lin, L. Zhang, N. Q. Pan, X. Cao and J. Li. "Photocatalytic Degradation of Methyl Orange Using a TiO<sub>2</sub>/Ti Mesh Electrode with 3D Nanotube Arrays", *Applied Material Interfaces*, vol. 4, pp. 171-177, 2012
- [10]. Z. Zhang, Y. Yu, and P. Wang."Hierarchical Top-Porous/Bottom-Tubular TiO<sub>2</sub> Nanostructures Decorated with Pd Nanoparticles for Efficient Photoelectrocatalytic Decomposition of Synergistic Pollutants", *ACS. Applied Mater Interface*, vol. 4, pp. 990-996, 2012
- [11]. Y. L. Pang, S. Lim, H. C. Ong and W. T. Chong. "Review A critical review on the recent progress of synthesizing techniques and fabrication of TiO<sub>2</sub> -based nanotubes photocatalysts", *Applied Catalysis A: General*, vol. 481, pp. 127-142, 2014
- [12]. J. Schneider, M. Matsuoka, M. Takeuchi, J. Zhang, Y. Horiuchi, M. Anpo and D. W. Bahnemann. "Understanding TiO<sub>2</sub> Photocatalysis: Mechanisms and Materials", *Chemical. Review*, vol. 114, pp. 9919-9986, 2014
- [13]. K. Lee, A. Mazare and P. Schmk. "One-Dimensional Titanium Dioxide Nanomaterials: Nanotubes", *Chemical Review*, vol. 114, pp. 9385-9454, 2014
- [14]. T. Toyada and Q. Shen. "Effect of Nanostructured TiO<sub>2</sub> Morphologies on Photovoltaic Properties." *Jornal of .Physical Chemistry Letter*, pp. 1885-1893, 2012.
- [15]. V. Zwilling, M. Aucouturier and E. Darque-Cerett. "Anodic oxidation of titanium and TA6Valloy in chromic media. An electrochemical approach", *Electrochimica Acta*, vol. 45, pp. 921-929, 1999.
- [16]. S. P. Albu and P. Schmuki. "Influence of anodization parameters on the expansion factor of TiO<sub>2</sub> nanotube", *Electrochem.Acta*, vol. 91, pp. 90-95, 2013
- [17]. D. B. Regonini. C. R. Bowen, A. Jaroenworalluck. and R. Stevens. "A review of growth mechanism, structure and crystallinity of anodized TiO<sub>2</sub> nanotubes", *Materials Science and Engineering*, vol. 74, pp. 377-406, 2013.
- [18]. M. Altomare, M. Pozzia, M. Allieta, L. G. Bettini and E. Sellì. "H<sub>2</sub> and O<sub>2</sub> photocatalytic production on TiO<sub>2</sub> nanotube arrays: Effect of the anodization time on structural features and photoactivity", *Applied Catalysis B: Environmental*, vol. 136, pp. 81-88, 2013
- [19]. M. Rani, S. J. Abbas and S. K Tripathi. "Influence of annealing temperature and organic dyes as sensitizers on sol-gel derived TiO<sub>2</sub> films", *Materials Science and Engineering:B*, vol. 187, pp. 75-82, 2014
- [20]. S. T. Kochuveedu, D. P. Kim and D. H. Kim. "Surface-Plasmon-Induced Visible Light Photocatalytic Activity of TiO<sub>2</sub> Nanospheres Decorated by Au Nanoparticles with Controlled Configuration", *Journal of Physical Chemistry C*, vol 116, pp. 2500-2506, 2012
- [21]. Ratnawati, J. Gunlazuardi, E. Listiani and Slamet. "Effect of NaBF<sub>4</sub> addition on the anodic synthesis of TiO<sub>2</sub> nanotube arrays photocatalyst for production of hydrogen from glycerol water solution", *International Journal of Hydrogen Energy*, vol. 39, pp.16927-16935, 2014.
- [22]. Pan. R, Wu.Y, Li.Z, and Fang.Z. "Effect of irradiation on deposition of CdS in fabricating coaxial hetrostructure of TiO<sub>2</sub> nanotube arrays via chemical deposition." *App.surf.scien*, vol. 292, pp. 886-891, 2014
- [23]. J. Luo, L. Ma, T. He, C. Fan Ng, S. Wang, H. Sun and H. J. Fan. "TiO<sub>2</sub>/(CdS, CdSe, CdSeS) Nanorod Heterostructures and Photoelectrochemical Properties", *Journal of Physical Chemistry. C*, vol 116, pp. 11956-11963, 2012
- [24]. K. Qing, S. Liu, L. Yang, Q. Cai, and C. A. Grimes. "Fabrication of PbS Nanoparticle-Sensitized TiO<sub>2</sub> Nanotube Arrays and Their Photoelectrochemical Properties", *ACS. Applied Materials Interfaces*, vol. 3, pp. 746-749, 2011
- [25]. H. Wang, W. Zhu, B. Chon and K. Qin. "Improvement of Photocatalytic Hydrogen Generation From CdSe/CdS/TiO<sub>2</sub> Nanotube-Arrays Coaxial Heterogeneous Structure", *International. Journal Hydrogen Energy*, vol. 39, pp. 90-91, 2014.
- [26]. Z. Pan, Y. Li, X. Hou, J. Yan and C. Wan. "Effect of Annealing Temperature on Photocatalytic Activity of CdS-modified TNAs/Glass Nanotube Arrays", *Physica E*, vol. 63, pp. 1-7, 2014.
- [27]. X. Zhang, S. Lin, J. Liao, N. Pan, D. Li and X. Cao. "Uniform deposition of water-soluble CdS quantum dots on TiO<sub>2</sub> nanotube arrays by cyclic voltammetric electrodeposition: Effectively prevent aggregation and enhance visible-light photocatalytic activity", *Electrochem.Acta*, vol. 108, pp. 296-303, 2013.
- [28]. M. E. Kern and D. F. Watson. "Influence of Solvation and the Persistence of Adsorbed Linkers on the Attachment of CdSe Quantum Dots to TiO<sub>2</sub> via Linker-Assisted Assembly", *Langmuir*, vol. 28, pp. 15598-15605, 2012
- [29]. Xie.Y, Ali. G, Yoo.S.W, and Cho.S.O, Sonication-Assisted Synthesis of CdS Quantum-Dot-Sensitized TiO<sub>2</sub> Nanotube Arrays with Enhanced Photoelectrochemical and Photocatalytic Activity, *Applid Material & Interfaces*, vol. 2, pp. 2910-2914, 2010.
- [30]. L. Sang, H. Tan, X. Zhang, Y. Wu, C. Ma and C. Burdha. "Effect of Quantum Dot Deposition on The Interfacial Flatband Potential, Depletion Layer in TiO<sub>2</sub> Nanonotube Electrodes, and Resulting H<sub>2</sub>

- Generation Rates”, *Journal of Physical Chemistry C*, vol 116, pp. 18633-18640, 2012
- [31]. L. Liu, J. Lv, G. Xu, Y. Wang, K. Xie, Z. Chan and Y. Wu. “Uniformly dispersed CdS nanoparticle sensitized TiO<sub>2</sub> nanotube arrays with enhanced visible-light photocatalytic activity and stability”, *Journal of Solid State Chemistry*, vol. 208, pp. 27-34, 2013.
- [32]. S.S. Kalanur, S. H. Lee, Y. J. Hwang and O. S. Joo. “Enhanced photoanode properties of CdS nanoparticle sensitized TiO<sub>2</sub> nanotube arrays by solvothermal synthesis”, *Journal of Photochemistry Photobiology A: Chemistry*, vol. 259, pp. 1-9, 2013